A diethyleneglycol-pyrene-modified Ru(II) catalyst for the design of buckypaper bioelectrodes and the wiring of glucose dehydrogenases

Luminita Fritea, Andrew James Gross, Bertrand Reuillard, Karine Gorgy, Serge Cosnier, Alan Le Goff

ARTICLE

A diethyleneglycol-pyrene-modified Ru(II) catalyst for the design of buckypaper bioelectrodes and the wiring of glucose dehydrogenases

Luminita Fritea,[a,b] Andrew J. Gross,[a] Bertrand Reuillard,[a] Karine Gorgy,[a] Serge Cosnier*[a] and Alan Le Goff*[a]

Abstract: A novel water-soluble Ru complex bearing phenanthrolinequinone ligands, diethyleneglycol linkers and pyrene anchoring groups was synthesized. Electrical wiring of NAD- and FAD-dehydrogenases is demonstrated via NADH oxidation and mediated electron transfer respectively. Bioelectrocatalysis is facilitated by the flexible and hydrophilic PEG groups, and strong binding of pyrene groups with the carbon nanotubes (CNTs) of the electrodes. Furthermore, owing to the surfactant properties of the PEG-modified complex, high quality CNT dispersions were obtained for homogeneous buckypaper preparation.

Introduction

Flavin adenine dinucleotide-dependent glucose dehydrogenase dehydrogenase (FAD-GDH) has been recently envisioned as a promising alternative for catalytic oxidation of glucose at the anode of enzymatic fuel cells (EFCs).[1–6] FAD-GDH offers important advantages as compared to the more extensively-studied NAD-dependent GDH or glucose oxidases (GOx).[7–12] On the contrary to GOx, FAD-GDH does not use O_2 as a co-substrate and therefore does not generate H_2O_2 which can inhibit cathodic enzymes and degrades biofuel cell performance.[8] Unlike NAD-GDH, NADH cofactor is not required for the oxidation of glucose with FAD-GDH because the FAD cofactor is tightly bound to the enzyme. However, the commercially-available fungal FAD-GDH is not easily wired at an electrode surface and therefore requires the use of an artificial redox mediator. Different types of redox partners have been investigated for the wiring of fungal FAD-GDH such as quinones,[11,13,14] polyoxometalates[15], osmium,[7,9,12,16] ruthenium[17] or iron complexes[8]. These redox partners have mainly been directly adsorbed on electrodes or covalently-attached to a polymer backbone.

Carbon nanotubes (CNTs) have been intensively studied in the design of EFC electrodes.[2,3,18–20] In particular, the emerging use of buckypaper (BP) electrodes has recently improved the processability and flexibility of CNT-based electrodes in the design of flexible and wearable EFCs.[21–26] BPs are commonly prepared from the filtration of a concentrated dispersion of surfactant-wrapped CNTs using a nonionic surfactant bearing PEG groups such as Triton X-100.[27] However, the presence of residual surfactant within the BP is highly undesirable for electrochemical applications as it will result in hindered conductivity and catalysis, as well as raising serious biocompatibility concerns.[26] Thus, surfactant-free methods have been developed, although dispersion quality can strongly vary depending on the type and concentration of CNTs used in the process.[13,28,29]

Taking advantage of the large specific surface area and high conductivity of CNT films, BPs also provide easily-scalable and flexible film-like electrodes with quasi-ideal properties for EFC applications.[26] Another great advantage of using CNTs is the large library of chemical modification strategies that have been made available for the functionalization of CNT sidewalls.[30,31] In particular, pi-pi stacking of pyrene molecules represents a reliable, soft and stable method for the non-covalent attachment of redox mediators and enzymes. A broad range of redox mediators have recently been modified with pyrene groups for stable attachment to CNTs while acting as a redox partner for enzyme wiring.[32–36]

Here we report the synthesis of an original Ru(II) complex bearing two phenanthrolinequinone (phendione) ligands and a bipyridine ligand substituted with a diethyleneglycol-type linker and a pyrene anchoring group (**RuPEG**). Multi-walled CNT (MWCNT) electrodes were first modified with this complex and then by either a FAD or NAD-dependent oxidoreductase enzyme. NAD-dependent dehydrogenase was used in a combined electroenzymatic process leading to NADH and glucose oxidation. The enzymes were chemically immobilized on MWCNTs through the formation of an amide linkage with 1-pyrenebutyric acid *N*-hydroxysuccinimide ester (pyreneNHS) (Figure 3A and 5A). Furthermore, a functional free-standing BP bioelectrode was designed by taking advantage of the surfactant properties of the **RuPEG** complex stemming from the hydrophilic diethyleneglycol chains and hydrophobic pyrene moieties present on the phendione ligand. The electrical wiring of FAD-GDH via **RuPEG** was studied and compared with a parent Ru complex lacking the PEG chains (**Ru2**).

Results and Discussion

The ligand and the complex **RuPEG** were synthesized following a multi-step procedure as described in Figure 1. All of the intermediates and the final complex were fully characterized by ^{1}H NMR and mass spectroscopy. The complex **RuPEG** was then immobilized on MWCNT electrodes via pi-pi stacking on CNT sidewalls by soaking the electrode in a solution of 2.5 mM **RuPEG** in DMF.

[a] Dr L. Fritea, Dr A. Gross, Dr. B. Reuillard, Dr K. Gorgy, Dr S. Cosnier and Dr A. Le Goff
Département de Chimie Moléculaire, DCM, Univ. Grenoble Alpes, CNRS, 38000 Grenoble, France.
E-mail: alan.le-goff@univ-grenoble-alpes.fr , serge.cosnier@univ-grenoble-alpes.fr

[b] Dr L. Fritea
Preclinical Disciplines Department, Faculty of Medicine and Pharmacy, University of Oradea, 10 Piata 1 Decembrie Street, 410073 Oradea, Romania.

Supporting information for this article is given via a link at the end of the document.

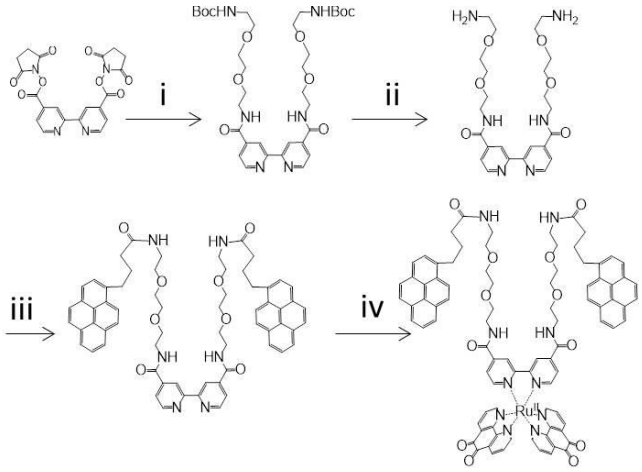

Figure 1. Synthesis of the complex **RuPEG:** (i) O-(2-Aminoethyl)-O′-[2-(Boc-amino)ethyl]diethylene glycol, Et_3N, DMF, 80°C, overnight, 69% (ii) trifluoroacetic acid (TFA), H_2O, triisopropylsilane (TIPS), RT, 30min, 100% (iii) Pyrene-NHS, Et_3N, DMF, 80°C, overnight, 88% (iv) $[Ru(Phendion)_2Cl_2]$, ethylene glycol, reflux, 1h, 54%

The immobilization of the **RuPEG** complex on MWCNT-coated glassy carbon (GC) electrodes was initially compared with the immobilization of the previously-described Ru(II) complex without the diethyleneglycol linker (complex **Ru2,** Figure 2).[37] The redox behavior of the modified electrode was characterized using cyclic voltammetry in 0.2 M potassium phosphate buffer, pH 7.0 (Figure 2).

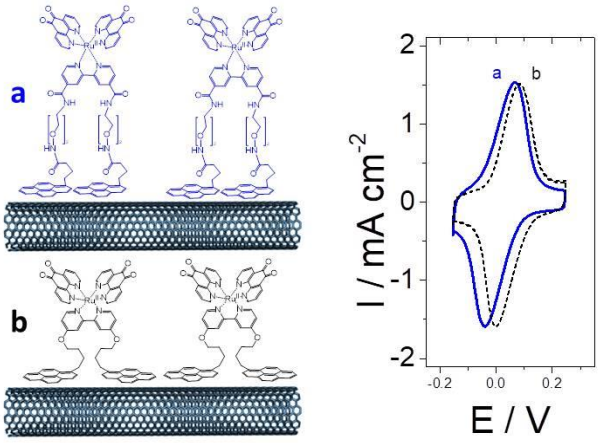

Figure 2. Cyclic voltammetry of (a) **RuPEG**- and (b) **Ru2**-functionalized MWCNT electrodes performed in 0.2 M PB (pH 7, 25°C, v = 10 mV s^{-1}) vs. Ag/AgCl. Experiments were performed on at least 3 three electrodes.

A reversible bielectronic peak system could be observed at +0.040 and +0.015 V vs. Ag/AgCl for **RuPEG**- and **Ru2**-functionalized MWCNT electrodes, respectively, corresponding to the two protons/two electrons (Q/QH_2) phendione ligands electroactivity in aqueous solution.[37–39] Oxidation and reduction peak currents remained highly stable upon multiple cyclic voltammetry (CV) scans (95% of the initial response retained after 100 cycles). The linear dependence of the peak currents towards the scan rate further confirmed the stable immobilization of both complexes on the MWCNT electrodes. Surface concentrations of 1.0 nmol cm^{-2} and 0.84 nmol cm^{-2}, for **RuPEG** and **Ru2** complexes, respectively, were estimated by integration of the charge under the anodic or the cathodic peak current. The similar surface concentration for the two types of functionalized electrode likely signifies a similar association constant for both complexes via pyrene-CNT interactions.[37]

Owing to the simple modification of MWCNTs using different types of pyrene derivatives,[37] a mixture of **RuPEG** and pyreneNHS (1:1 ratio) was explored to perform the double functionalization of CNTs and allow the covalent attachment of the enzyme via amide coupling. In the first approach, NAD-dependent GDH was combined with the Ru(II) catalyst and compared with the previously-designed bioelectrodes based on **Ru2** (Figure 3). [37]

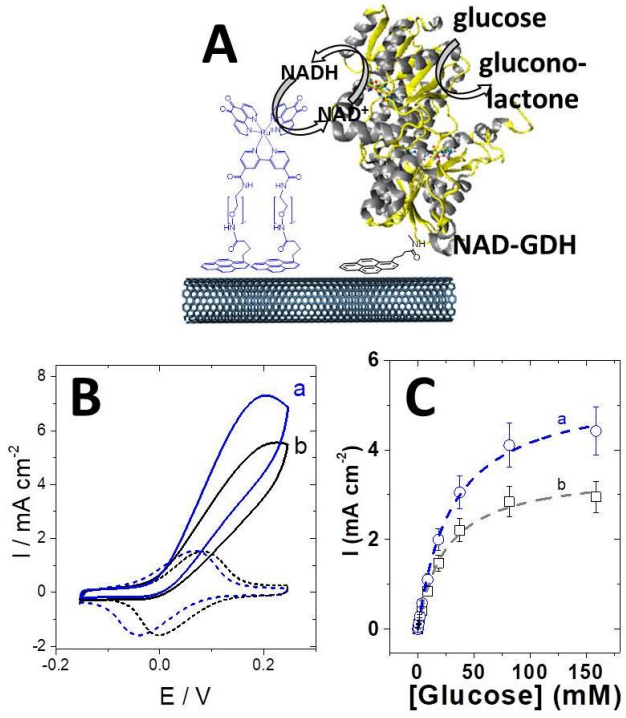

Figure 3. (A) Schematic representation of the **RuPEG**-functionalized MWCNT electrode with immobilized NAD-GDH. (B) Cyclic voltammograms of (a) **RuPEG**- and (b) **Ru2**-functionalized MWCNT electrodes with immobilized NAD-GDH in the absence (dashed line) and presence (solid line) of glucose (160 mmol L^{-1}) in phosphate buffer (0.2 M, pH 7) containing 10 mM NAD^+ at 37°C (v = 10 mV s^{-1}). (C) Calibration curve for glucose between 0 and 160 mmol L^{-1} and Michaelis-Menten-type fitting model (dashed line) for (a) **RuPEG** and (b) **Ru2** MWCNT electrodes. Applied potential 0.15 V vs. Ag/AgCl. Experiments were performed on at least 3 three electrodes. The error bars correspond to the standard deviation.

CV experiments were recorded in the presence of 160 mM glucose and 10 mM of NAD^+ for **RuPEG**- and **Ru2**-functionalized MWCNT electrodes with immobilized NAD-GDH (Figure 3B). In the presence of glucose, an electrocatalytic wave appears at an onset potential of -0.05 V vs. Ag/AgCl and corresponds to the oxidation of NADH, enzymatically generated via the oxidation of glucose by the grafted NAD-GDH. Chronoamperometric measurements were performed at 0.15 V vs. Ag/AgCl after successive addition of increasing glucose concentrations. A typical Michaelis-Menten dependence is observed, reaching maximum catalytic currents of 4.5 mA cm^{-2} (K_M = 30 mM) and 3.1 mA cm^{-2} (K_M = 25 mM) at 160 mM glucose under hydrodynamic conditions for **RuPEG**- and **Ru2**-functionalized MWCNT electrodes, respectively. Considering that similar amounts of **RuPEG** and **Ru2** are immobilized on the MWCNT electrodes, these experiments show that a ~50 % increase of electrocatalytic current density is observed with the **RuPEG** electrode. This can be explained by the higher solvation and flexibility of the diethyleneglycol derivative which facilitates the electrocatalytic activity of **RuPEG** towards NADH oxidation.

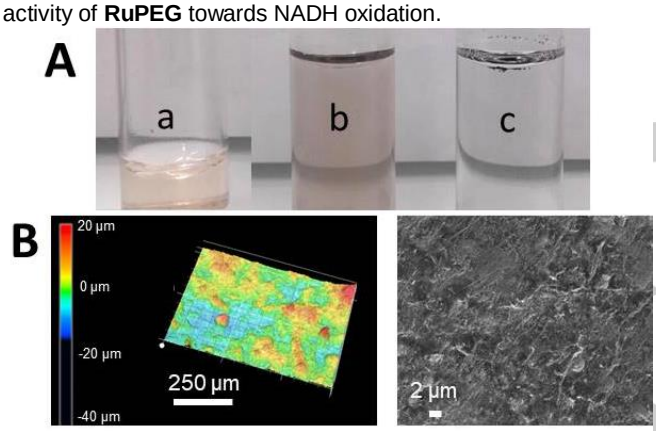

Figure 4. (A) Photographs of supernatant aqueous solutions obtained from dispersions after centrifugation of (a) **RuPEG**, (b) MWCNT+**RuPEG** and (c) MWCNT; (B) LSM and SEM images of the **RuPEG**-functionalized BP

The properties of **RuPEG** as a MWCNT surfactant were also investigated to facilitate the preparation of functionalized CNT dispersions and the fabrication of BPs. This configuration was also studied in order to address the ability of **RuPEG** to act as a redox mediator for FAD-GDH, co-immobilized via the pyreneNHS linker. As shown in Figure 4A, the addition of **RuPEG** to a suspension of MWCNTs improved the dispersion of MWCNTs after sonication for 10 min and centrifugation, underlining the surfactant properties of the Ru complex towards MWCNTs. Improved solubility of modified CNTs has already been demonstrated using polypyridyl-ruthenium complexes bearing pi-extended ligands[40] and pyrene anchors[41] but never with a diethyleneglycol chain which can improve the hydrophilicity and biocompatibility of the formed CNT composite. Thus, highly stable and flexible BPs could be obtained following vacuum filtration of a 6 mg mL^{-1} **RuPEG**-modified MWCNTs dispersion onto a PTFE membrane. Laser scanning microscopy (LSM) and scanning electron microscopy (SEM) images, respectively, demonstrated homogeneity of the BP surface at the macroscale and a typical dense, intimately-intricate network of MWCNTs at the nanoscale (Figure 4B). The homemade BPs had thicknesses of 180 (±10) µm and were accompanied with reasonable conductivities of 6 (±1) S cm^{-1}. These characterization experiments indicate the formation of a well-defined free-standing MWCNT film due to the presence of **RuPEG**.

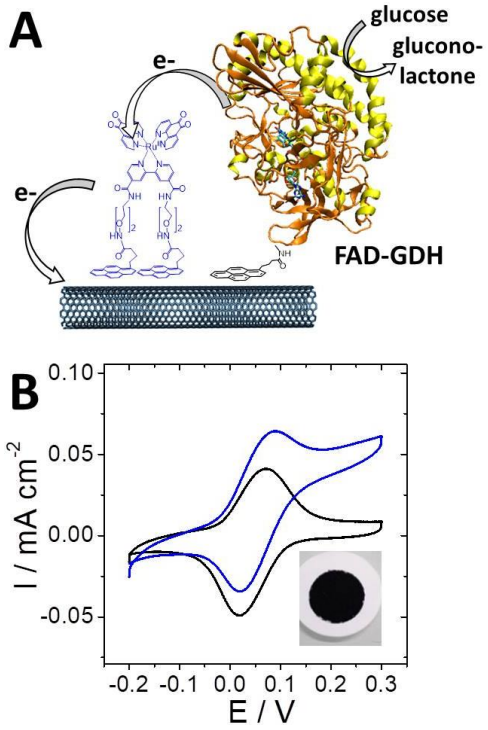

Figure 5. (A) **RuPEG**-functionalized MWCNT electrode with immobilized FAD-GDH. (B) CVs of **RuPEG**-functionalized BP in the absence (black line) and presence (blue line) of glucose (150 mmol L^{-1}) in PB (0.2 M, pH 7, 25°C, v = 1 mV s^{-1}) vs. Ag/AgCl; inset: photograph of the **RuPEG**-functionalized BP. Experiments were performed on three electrodes.

Following the immobilization of the FAD-GDH on the **RuPEG**-functionalized homemade BP, CV experiments performed in the presence of glucose revealed a clear electrocatalytic wave starting at -0.1 V vs. Ag/AgCl (Figure 5B). The latter was ascribed to a mediated electron transfer (MET)-based bioelectrocatalytic oxidation of glucose by the FAD-GDH that is able to directly transfer electrons to the quinone moieties of **RuPEG**. A maximum current density of 0.06 mA cm^{-2} could be reached at 0.2 V vs. Ag/AgCl. These results demonstrate that diethyleneglycol -based Ru complexes can not only be used as redox mediators for FAD-GDH, but also as CNT surfactants for the fabrication of robust BP electrodes.

In order to benchmark this homemade BP electrode, we also investigated the modification of a commercially available MWCNT BP (from NanoTechLabs Inc) with the **RuPEG** catalyst and the

FAD-GDH enzyme. The non-covalent modification was performed by first drop coating 40 µL of a 1:1 mixture of **RuPEG** and pyreneNHS at 2.5 mM in DMF onto a 6 mm diameter BP disk followed by drop coating of a 2.5 mg mL^{-1} of FAD-GDH in phosphate buffer at pH7. LSM and SEM images presented in Figure 6A show homogeneity of the commercial BP surface at the macroscale and a significantly more porous MWCNTs network with pores of larger diameters than the **RuPEG** modified homemade BP (Figure 4). Figure 6B shows CV scans for the commercial BP electrodes modified with **Ru2** and **RuPEG**, after the immobilization of FAD-GDH, in the absence and presence of glucose. In the presence of the enzyme's substrate, a bioelectrocatalytic wave is observed for both BP bioelectrodes with an onset potential of about -0.15 V vs. Ag/AgCl. Maximum current densities of 0.095 and 1.36 mA cm^{-2} were obtained at 0.2 V with 150 mmol L^{-1} glucose for **Ru2** and **RuPEG**-modified BP, respectively. These results confirm that **RuPEG** can act as an efficient redox mediator for glucose oxidation by FAD-GDH. Furthermore, the large difference of catalytic current density observed between **RuPEG** and **Ru2** modified BP highlights the crucial finding that the PEG chain readily improves the electrical wiring of the FAD-GDH enzyme to the electrode surface. This enhanced wiring effect observed with **RuPEG** can be attributed in part to the improved flexibility of the PEG chain that helps to promote electronic communication with the buried FAD site. The strong influence of the chain length over the MET efficiency, and the importance of having a flexible linker, have already been demonstrated by different groups in the engineering of osmium hydrogels for the wiring of glucose oxidases and multicopper enzymes[42] or ferrocene-PEG derivatives for the mediated oxidation of NADH,[43,44] but not for the emerging FAD-GDH enzyme. The higher performances observed at the **RuPEG**-functionalized commercial BP (1.36 mA cm^{-2}) compared to the **RuPEG**-modified homemade BP (0.06 mA cm^{-2}) may be attributed to the limited interaction between the Ru complex and the enzyme in the more compact homemade BP structure. The difference in the type of CNTs used, a mixture of ca 5 nm and ca 80 nm diameter MWCNTs, may also contribute to the improved catalytic performance observed with the commercial BP electrodes, for example, via hierarchical porosity effects. Moreover, the diethyleneglycol groups provide regions of hydrophilicity at the electrode which, when combined with the "open" porous structure of commercial BP, facilitate enzyme immobilization. Overall, these experiments demonstrate that the **RuPEG**-modified commercial BP electrode combines the advantages of an efficient redox mediator within a porous environment thus optimizing the electrical wiring of the FAD-GDH and the diffusion of glucose.

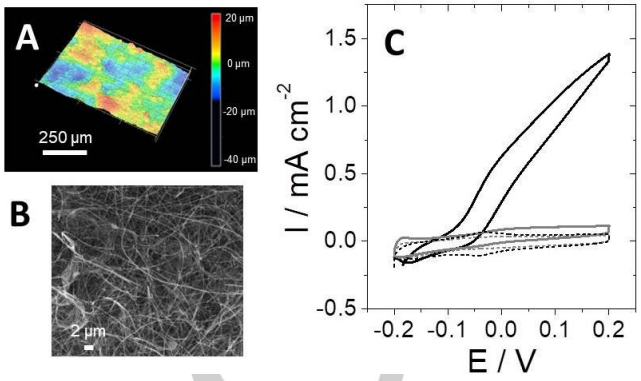

Figure 6. (A) LSM and SEM images of the **RuPEG**-functionalized commercial BP (B) Cyclic voltammograms of commercial BP bioelectrodes functionalized with pyreneNHS/FAD-GDH and **Ru2** (gray lines) or **RuPEG** (black lines) complexes in the absence (dashed line) and presence (solid line) of 150 mmol L^{-1} glucose in PB (0.2 M, pH 7, 25°C, v = 1 mV s^{-1}) vs. Ag/AgCl. Experiments were performed on at least 3 three electrodes.

Conclusions

This work underlines the benefit of molecularly engineering redox centers for the wiring of redox enzymes confined at porous electrode surfaces. The multifunctional ruthenium complex bearing pyrene-terminated diethyleneglycol chains, **RuPEG,** allowed for the simple functionalization of CNT-coated and BP-based electrodes while generating an efficient redox wiring of NAD- and FAD-dependent dehydrogenases for glucose oxidation. In the general context of the development of enzyme based bioelectrodes, this strategy of rationally designing single-molecule redox centers stands as a viable alternative to the use of redox hydrogels for efficient redox enzyme wiring. This type of versatile transition-metal complex bearing pyrene-terminated polyethyleneglycol-type chains could be extended to other types of enzymes and redox partners for the building of robust and catalytically powerful bioelectrodes. Future work will focus on the optimization of the loading of the enzyme and the redox mediators in buckypapers to further increase current densities.

Experimental Section

Materials and methods

All chemical products were purchased from Sigma Aldrich. Fungal flavin adenine dinucleotide-dependent glucose dehydrogenase (FAD-GDH, 1150 U mg^{-1} solid) was purchased from Sekisui Diagnostics (UK). NAD-dependent GDH from *Pseudomonas sp.* (235 U mg^{-1}) was purchased from Aldrich. Commercial grade thin multi-walled carbon nanotubes (MWCNTs, 9.5 nm diameter, purity > 95%, 1.5 µm length) were obtained from Nanocyl. Commercial MWCNT proprietary blend buckypaper with reference (NTL-12218, 60 gsm) was obtained from NanoTechLabs, Inc (Buckeye Composites). Carbon nanomaterials were used as received without any purification. When not used, the enzyme was stored at -20°C. All the reagents

were used without further purification. All solvents were of analytical grade. Distilled water was passed through a Milli-Q water purification system to obtain ultrapure water at 18.2 MΩ cm^{-1}. Glucose solutions were left to mutarotate overnight to β-D-glucose prior to use. 3D and profile images were taken using a Keyence VK-X200 laser microscope. 0.1 M, pH 7 phosphate buffer solution was prepared from Milli-Q water.

NMR spectra were recorded on a Bruker AVANCE 400 operating at 400.0 MHz for 1H. ESI mass spectra were recorded with a Bruker APEX-Qe ESI FT-ICR mass spectrometer.

Conductivity measurements were performed using a Keithley 2450 sourcemeter with an S-302-4 mounting stand and SP4 four-point probe head, taking into account the thickness of each sample. 6 measurements were recorded per sample from a minimum of 2 independent samples.

Electrochemical measurements

The electrochemical experiments were carried out in a three electrode electrochemical cell using an Autolab PGSTAT100 potentiostat and a Biologic VMP3 Multi Potentiostat. A Pt wire was used as the counter electrode and the Ag/AgCl (KCl sat.) served as the reference electrode. All experiments were conducted at room temperature in air. All current densities are normalized towards the geometrical surface of the electrode. All simulated curves were obtained via Origin Pro 9.0.

Synthesis

$[Ru(Phendion)_2Cl_2]$ and (1,10-phenathroline-5,6-dione)$_2$((4,4'-bis(4-pyrenyl-1-ylbutyloxy)-2,2'-bipyridine) Ru(II)] $(PF_6)_2$) **Ru2** were synthesized according to previously described procedures[37,38,45,46].

BpyPEG-NHBOC: A solution of 100 mg of 1,1'-[2,2'-Bipyridine-4,4'-diylbis(carbonyloxy)]di(2,5-pyrrolidinedione) in 4 mL DMF was slowly added to a solution of 0.11 mL of O-(2-Aminoethyl)-O′-[2-(Boc-amino)ethyl]diethylene glycol (2 eq) and 0.08 mL Et_3N (3 eq) in 8 mL DMF . The mixture was stirred overnight at 80°C. The solvent was evaporated and the crude product was washed twice with H_2O and Et_2O, affording a white powder (111 mg, 69 % yield).

^{1}H NMR: δ_H/ppm (400 MHz, DMSO): 1.35 (s, 18H, 6 x CH_3), 3.06 (m, 4H, 2 CH_2), 3.40 (m, 4H, 2 CH_2), 3.46-3.58 (m, 16 H, 8 x CH_2), 6.71 (m, 2H, NH), 7.85 (m, 2H, NH), 8.82 (m, 2H, bpy), 8.87 (m, 2H, bpy), 9.00 (m, 2H, bpy)

BpyPGE-NH_2: A solution of 50 mg of BpyPEG-NHBOC and 9.5 mL of TFA (95 %) was prepared in 0.25 mL of H_2O and 0.25 mL of TIPS. The mixture is stirred at room temperature for 30 min. The solvent is evaporated and the crude oil is washed twice with Et_2O, affording 35 mg of BpyPGE-NH_2 (100 % yield). ^{1}H NMR: δ_H/ppm (400 MHz, DMSO): 2.97 (m, 4H, 2 CH_2), 3.49 (m, 4H, 2 CH_2), 3.60 (m, 16 H, 8 x CH_2), 7.73 (m, 4H, NH_2), 7.86 (m, 2H, NH), 8.79 (m, 2H, bpy), 8.87 (m, 2H, bpy), 9.00 (m, 2H, bpy) ; MS (ESI$^+$): 253.2 (BpyPEG-$(NH_3^+)_2$)

BpyPEG-pyrene: A solution of 55 mg of pyrene-NHS in 3 ml DMF was slowly added to a mixture of 36 mg of BpyPGE-NH_2 and 0.03 mL Et_3N (3 eq). The mixture is stirred overnight at 80°C. The DMF is evaporated and the crude product is washed with H_2O and Et_2O, yielding 66 mg of a light-brown powder (88% yield). ^{1}H NMR: δ_H/ppm (400 MHz, DMSO): 1.97 (m, 4H, 2x CH_2), 2.22 (m, 4H, 2 x CH_2), 3.24 (m, 8H, 4 x CH_2), 3.43 (m, 8 H, 4 x CH_2), 3.53 (m, 12 H, 6 x CH_2), 7.82 (m, 4H), 7.90 (m, 2H), 8.01 (m, 2H), 8.05 (m, 4H), 8.18 (m, 4H), 8.34 (m, 2H), 8.76 (m, 2H), 8.82 (m, 2H), 8.95 (m, 2H) ; MS (ESI+): 1045.7

*Complex **RuPEG**:* A solution of BpyPEG-pyrene (53mg) and $[Ru(Phendion)_2Cl_2]$ (30 mg) in ethylene glycol (3 mL) was refluxed for 1 h under argon. After cooling down to room temperature, a 10mL aqueous solution of saturated NH_4PF_6 was added, allowing the as-formed product to precipitate. The orange brown precipitate was filtrated, then washed with water and Et_2O, yielding 53 mg of product (54% yield).^{1}H NMR: δ_H/ppm (400 MHz, DMSO): 1.88 (m, 8H, 4 x CH_2), 2.22 (m, 4H, 2 x CH_2), 3.20 (m, 8H, 4 x CH_2), 3.40 (m, 20 H, 10 x CH_2), 7.50 (m, 4H), 7.70 (m, 6H), 8.01 (m, 14H), 8.36 (m, 6H), 8.37 (m, 2H), 8.47 (m, 2H), 8.97 (m, 2H); MS (ESI$^+$): 783.1 (M-2PF_6^{2+})

Fabrication of the MWCNT-coated GC electrodes

The MWCNT-coated electrodes were obtained by drop casting 20 µL of a MWCNT dispersion in 1-methyl-2-pyrrolidinone (NMP) (5 mg mL^{-1}) onto polished glassy carbon (GC) rod electrodes (3 mm diameter), affording a 5-µm–thick homogeneous MWCNT film on the GC electrode.

The **RuPEG**/GDH and **Ru2**/GDH MWCNT enzyme-modified electrodes were prepared by a first incubation step in a 1:1 ratio of 2.5 mM **RuPEG**/Pyrene-NHS in DMF. After solvent removal under vacuum, the bi-functionalized electrodes were then incubated for at least 6 h in 20 µL of a 2.5 mg mL^{-1} solution of GDH in phosphate buffer pH 7 at 4°C.

After each incubation, the electrodes were rinsed several times with deionized water.

Preparation of commercial BP modified with pyreneNHS, RuPEG and FAD-GDH (drop-casting only)

For preparation of the **RuPEG**-based commercial BP, high conductivity MWCNT buckypaper from NanoTechLabs Inc was first cut into 6 mm diameter circular disk electrodes. Next, 40 µL of 2.5 mmol L^{-1} **RuPEG**/pyrene-NHS (1:1) in DMF was drop-coated onto the electrode and left to dry overnight at room temperature. For enzyme immobilization, 40 µL of 2.5 mg mL^{-1} FAD-GDH in 0.1 mol L^{-1} PB pH 7 was drop-casted onto the electrode then dried overnight in the fridge. Electrical contact to the BP was obtained via a metal wire with carbon paste. The back and sides of the electrode were sealed with silicone paste. The electrodes were rinsed several times with deionized water before use.

Preparation of homemade BP from a MWCNT dispersion modified with pyreneNHS, RuPEG and FAD-GDH (bulk functionalization and drop-casting)

For preparation of the **RuPEG**-based homemade BP, 6 mg of MWCNTs was added into 3 mL of DMF and dispersed by 60 min sonication using a Bandelin sonorex RK100 ultrasonication bath. Next, **RuPEG**/pyrene-NHS (1:1, 250 µmol L^{-1}) were added into the dispersion and the resulting mixture was agitated by hand and vortex for 10 min. The dispersion was subsequently passed through a Millipore PTFE filter (JHWP, 0.45 µM pore size) under high vacuum using a MZ 2C NT Vacuubrand GMBH membrane pump, rinsed with ultrapure water, then left under vacuum for a further 30-60 min. The BP coated filter papers were left overnight, peeled off the filter to obtain the free-standing BP, then cut into 6 mm diameter circular disk electrodes. For enzyme immobilization,

40 µL of 2.5 mg mL^{-1} FAD-GDH in 0.1 mol L^{-1} PB pH 7 was drop-casted onto the electrode then dried overnight in the fridge. The electrodes were rinsed several times with deionized water before use.

Acknowledgements

This work was supported by the Labex ARCANE ((ANR-11-LABX-0003-01) and the Graduate School on Chemistry, Biology and Health of Univ Grenoble Alpes CBH-EUR-GS (ANR-17-EURE-0003). The authors wish to acknowledge the platform Chimie NanoBio ICMG FR 2607 (PCN-ICMG) and Yannig Nedellec for BP conductivity measurements. SEM was performed at the CMTC characterization platform of Grenoble INP supported by the Centre of Excellence of Multifunctional Architectured Materials "CEMAM" n°AN-10-LABX-44-01 funded by the "Investments for the Future" Program.

Keywords: glucose • biofuel cell • ruthenium complex • carbon nanotubes • pyrene

[1] A. Le Goff, M. Holzinger, *Sustainable Energy Fuels* **2018**, *2*, 2555–2566.
[2] S. Cosnier, A. J. Gross, A. Le Goff, M. Holzinger, *Journal of Power Sources* **2016**, *325*, 252–263.
[3] M. Rasmussen, S. Abdellaoui, S. D. Minteer, *Biosens. Bioelectron.* **2016**, *76*, 91–102.
[4] E. Katz, K. MacVittie, *Energy Environ. Sci.* **2013**, *6*, 2791–2803.
[5] S. C. Barton, J. Gallaway, P. Atanassov, *Chem. Rev.* **2004**, *104*, 4867–4886.
[6] D. Leech, P. Kavanagh, W. Schuhmann, *Electrochim. Acta* **2012**, *84*, 223–234.
[7] M. N. Zafar, N. Beden, D. Leech, C. Sygmund, R. Ludwig, L. Gorton, *Anal. Bioanal. Chem.* **2012**, *402*, 2069–2077.
[8] R. D. Milton, F. Giroud, A. E. Thumser, S. D. Minteer, R. C. T. Slade, *Phys. Chem. Chem. Phys.* **2013**, *15*, 19371–19379.
[9] S. Tsujimura, K. Murata, W. Akatsuka, *J. Am. Chem. Soc.* **2014**, *136*, 14432–14437.
[10] D. MacAodha, P. O. Conghaile, B. Egan, P. Kavanagh, C. Sygmund, R. Ludwig, D. Leech, *Electroanalysis* **2013**, *25*, 94–100.
[11] C. Hou, Q. Lang, A. Liu, *Electrochimica Acta* **2016**, *211*, 663–670.
[12] K. Murata, W. Akatsuka, T. Sadakane, A. Matsunaga, S. Tsujimura, *Electrochim. Acta* **2014**, *136*, 537–541.
[13] Andrew. J. Gross, X. Chen, F. Giroud, C. Abreu, A. Le Goff, M. Holzinger, S. Cosnier, *ACS Catal.* **2017**, *7*, 4408–4416.
[14] N. Tsuruoka, T. Sadakane, R. Hayashi, S. Tsujimura, *International Journal of Molecular Sciences* **2017**, *18*, 604.
[15] F. Boussema, A. J. Gross, F. Hmida, B. Ayed, H. Majdoub, S. Cosnier, A. Maaref, M. Holzinger, *Biosens Bioelectron* **2018**, *109*, 20–26.
[16] P. Pinyou, A. Ruff, S. Poeller, S. Ma, R. Ludwig, W. Schuhmann, *Chem.-Eur. J.* **2016**, *22*, 5319–5326.
[17] R. Sakuta, K. Takeda, T. Ishida, K. Igarashi, M. Samejima, N. Nakamura, H. Ohno, *Electrochemistry Communications* **2015**, *56*, 75–78.
[18] S. Cosnier, M. Holzinger, A. Le Goff, *Front. Bioengineer. Biotechnol.* **2014**, *2*, 45.
[19] A. Le Goff, M. Holzinger, S. Cosnier, *Cell. Mol. Life Sci.* **2015**, *72*, 941–952.
[20] M. Holzinger, A. Le Goff, S. Cosnier, *Electrochim. Acta* **2012**, *82*, 179–190.
[21] D. V. Pankratov, Y. S. Zeifman, O. V. Morozova, G. P. Shumakovich, I. S. Vasil'eva, S. Shleev, V. O. Popov, A. I. Yaropolov, *Electroanalysis* **2013**, *25*, 1143–1149.
[22] L. Hussein, S. Rubenwolf, F. von Stetten, G. Urban, R. Zengerle, M. Krueger, S. Kerzenmacher, *Biosens Bioelectron* **2011**, *26*, 4133–4138.
[23] V. Scherbahn, M. T. Putze, B. Dietzel, T. Heinlein, J. J. Schneider, F. Lisdat, *Biosens. Bioelectron.* **2014**, *61*, 631–638.
[24] G. Strack, S. Babanova, K. E. Farrington, H. R. Luckarift, P. Atanassov, G. R. Johnson, *J. Electrochem. Soc.* **2013**, *160*, G3178–G3182.
[25] Y. Umasankar, D. B. Brooks, B. Brown, Z. Zhou, R. P. Ramasamy, *Adv. Energy Mater.* **2014**, *4*, 1301306.
[26] A. J. Gross, M. Holzinger, S. Cosnier, *Energy Environ. Sci.* **2018**, *11*, 1670–1687.
[27] L. Hussein, S. Rubenwolf, F. von Stetten, G. Urban, R. Zengerle, M. Krueger, S. Kerzenmacher, *Biosensors and Bioelectronics* **2011**, *26*, 4133–4138.
[28] X. Chen, A. J. Gross, F. Giroud, M. Holzinger, S. Cosnier, *Electroanalysis* **2018**, *30*, 1511–1520.
[29] B. Reuillard, J. Warnan, J. J. Leung, D. W. Wakerley, E. Reisner, *Angewandte Chemie International Edition* **2016**, *55*, 3952–3957.
[30] P. Singh, S. Campidelli, S. Giordani, D. Bonifazi, A. Bianco, M. Prato, *Chem. Soc. Rev.* **2009**, *38*, 2214–2230.
[31] N. Karousis, N. Tagmatarchis, D. Tasis, *Chem. Rev.* **2010**, *110*, 5366–5397.
[32] A. Le Goff, F. Moggia, N. Debou, P. Jegou, V. Artero, M. Fontecave, B. Jousselme, S. Palacin, *J. Electroanal. Chem.* **2010**, 57–63.
[33] N. Lalaoui, B. Reuillard, C. Philouze, M. Holzinger, S. Cosnier, A. Le Goff, *Organometallics* **2016**, *35*, 2987–2992.
[34] M. Bourourou, K. Elouarzaki, M. Holzinger, C. Agnès, A. Le Goff, N. Reverdy-Bruas, D. Chaussy, M. Party, A. Maaref, S. Cosnier, *Chem. Sci.* **2014**, *5*, 2885–2888.
[35] M. Bourourou, M. Holzinger, K. Elouarzaki, A. Le Goff, F. Bossard, C. Rossignol, E. Djurado, V. Martin, D. Curtil, D. Chaussy, et al., *Chem. Commun.* **2015**, *51*, 14574–14577.
[36] F. Giroud, R. D. Milton, B.-X. Tan, S. D. Minteer, *ACS Catal.* **2015**, *5*, 1240–1244.
[37] B. Reuillard, A. Le Goff, S. Cosnier, *Chem. Commun.* **2014**, *50*, 11731–11734.
[38] C. A. Goss, H. D. Abruna, *Inorg. Chem.* **1985**, *24*, 4263–4267.
[39] B. Reuillard, A. Le Goff, S. Cosnier, *Anal. Chem.* **2014**, *86*, 4409–4415.
[40] D. Jain, A. Saha, A. A. Martí, *Chemical Communications* **2011**, *47*, 2246–2248.
[41] K. Huang, A. Saha, K. Dirian, C. Jiang, P.-L. E. Chu, J. M. Tour, D. M. Guldi, A. A. Martí, *Nanoscale* **2016**, *8*, 13488–13497.
[42] F. Mao, N. Mano, A. Heller, *J. Am. Chem. Soc.* **2003**, *125*, 4951–4957.
[43] N. Allali, V. Urbanova, M. Etienne, X. Devaux, M. Mallet, B. Vigolo, J.-J. Adjizian, C. P. Ewels, S. Oberg, A. V. Soldatov, et al., *Beilstein J Nanotechnol* **2018**, *9*, 2750–2762.
[44] V. Urbanová, N. Allali, W. Ghach, V. Mamane, M. Etienne, M. Dossot, A. Walcarius, *Journal of Electroanalytical Chemistry* **2013**, *707*, 129–133.
[45] A. Le Goff, K. Gorgy, M. Holzinger, R. Haddad, M. Zimmerman, S. Cosnier, *Chemistry – A European Journal* **2011**, 10216–10221.
[46] F. Grimm, K. Hartnagel, F. Wessendorf, A. Hirsch, *Chem. Commun.* **2009**, 1331–1333.

Entry for the Table of Contents (Please choose one layout)

Layout 1:

ARTICLE

Text for Table of Contents

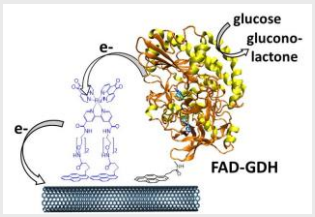

*Author(s), Corresponding Author(s)**

Page No. – Page No.

Title

Layout 2:

ARTICLE

((Insert TOC Graphic here))

*Author(s), Corresponding Author(s)**

Page No. – Page No.

Title

Text for Table of Contents